Supporting Information

Molecular Dynamics Simulations of Supramolecular Anticancer Nanotubes

Myungshim Kang[†], Kaushik Chakraborty[†], Sharon M. Loverde[†§*]

[†] Department of Chemistry, College of Staten Island, The City University of New York, 2800 Victory Boulevard, Staten Island, New York 10314, United States

[§] Ph.D. Program in Chemistry, Biochemistry, and Physics, The Graduate Center of the City University of New York, New York, New York 10016, United States

*Corresponding author: Sharon M. Loverde, Sharon.loverde@csi.cuny.edu

1. Simulation methods

Simulation systems. qCPT-buSS-Tau consists of four camptothecin (CPT) drugs and β-sheet forming peptide (CGVQIVYKK or Tau), which are conjugated via a biodegradable disulfide linker (buSS) (Figure S1). qCPT-buSS-Tau self-assembles into a nanotube, while mCPT-buSS-Tau forms a nanofilament. We built 7 preassembled systems with varying numbers of DAs per layer, conformation of DA and temperature, as summarized in Table S1. For instance, in the preassembled system 2, 12 DAs are placed in the first layer, as shown in Figure S2. The CPTs are pointing inward and an angle between the neighboring DAs is 30˚. The second layer has also 12 DAs and is rotated 15˚ relative to the first layer. The resulting nanotube has 6 layers with the inter-layer distance of 20 Å. The initial width of the nanotube is 115 Å. In total, it has 72 DAs. Each system is neutralized with Cl^- ions. After the solvation, it has 200,922 atoms in a box of 140x140x105 $Å^3$. The concentration of the DA is 58.3 mM. As summarized in Table S1, four more preassembled systems are explored. But, this report focuses on the preassembled system 2 for the reasons discussed later. A random system has 96 DAs (22.1mM) in a box of 193 x 193 x 193 $Å^3$ with 703,575 atoms in total.

Simulation methods. qCPT-buSS-Tau is parametrized using General AMBER force field (GAFF)[1]. Partial charges are assigned by Vcharge v1.01[2]. The TIP3P model is used for water[3]. Atomistic MD simulations are carried out using NAMD2.11[4]. All systems use the NPT ensemble and Langevin dynamics[5] at a pressure of 1 atm using Langevin piston method[5-6] with a piston period of 200 fs and a damping time scale of 50 fs at a temperature of 310 K with a damping coefficient $\gamma = 1\ ps^{-1}$. Full electrostatic interactions are taken into account, using the particle mesh Ewald (PME) algorithm[7], with full periodic boundary conditions. The cutoff for van der Waals interactions is 12 Å with a smooth switching function at 10 Å used to truncate the van der Waals potential energy at the cutoff distance. Covalent bonds involving hydrogen are held rigid using the SHAKE algorithm[8-9], which allows a 2 fs time step. Coordinates are saved every 2 ps for the post-analysis of the trajectory. Simulations are performed for ~400 and 300 ns, for the preassembled systems and the random system, respectively.

Due to the significant differences between the two systems, especially in the stacking of CPTs, another system is introduced: the preassembled system 5 is branched out from the preassembled system 4 after 120 ns simulation at 310 K and then the temperature is elevated to 350 K for 420ns to expedite the relaxation. We hypothesis that the preassembled system 2 with stronger stacking is closer to the equilibrated state than the preassembled system 4, and, therefore, with the elevated temperature the preassembled system 5 would move toward to the preassembled system 2.

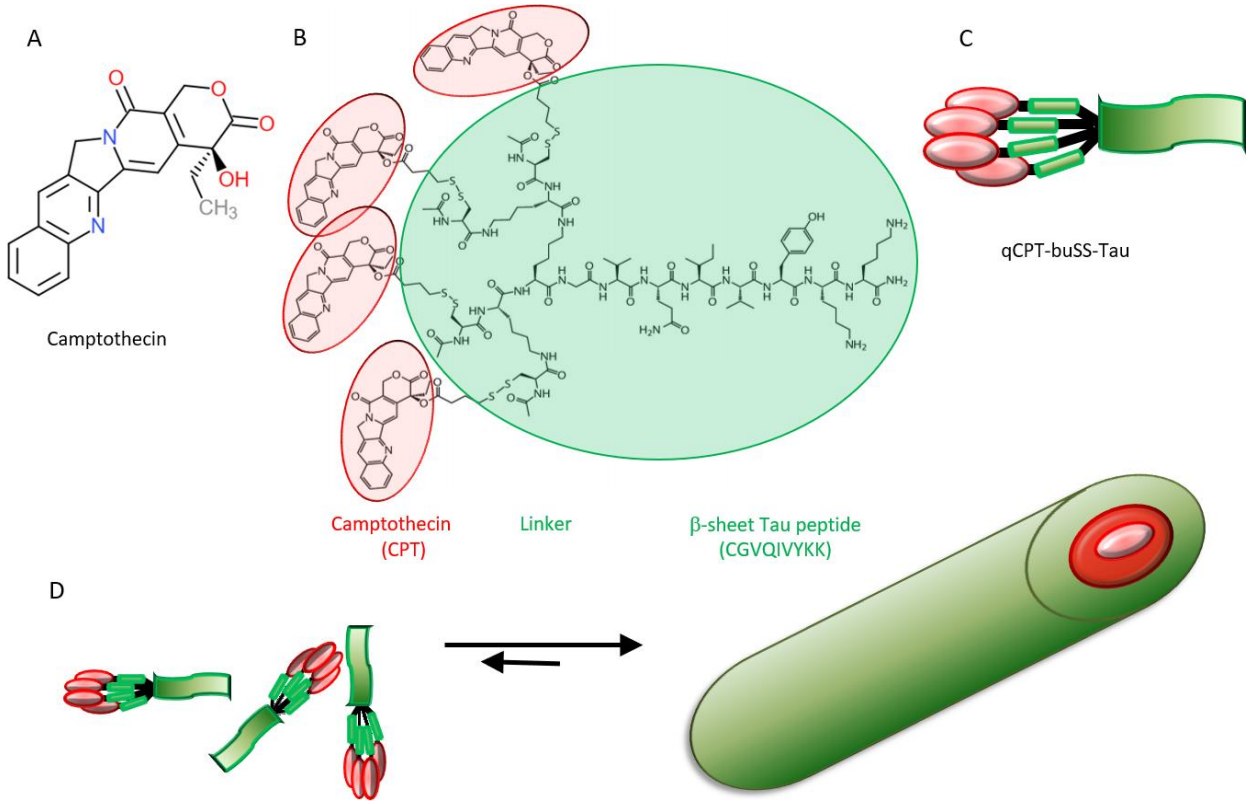

Figure S 1. DA of qCPT-buSS-Tau. A. Structure of camptothcin (CPT). B. Structure of qCPT-buSS-Tau. The four CPTs are in red, while the peptide and linker parts are in green. C. Schematic representation of qCPT-buSS-Tau. D. Self-assembly of DA.

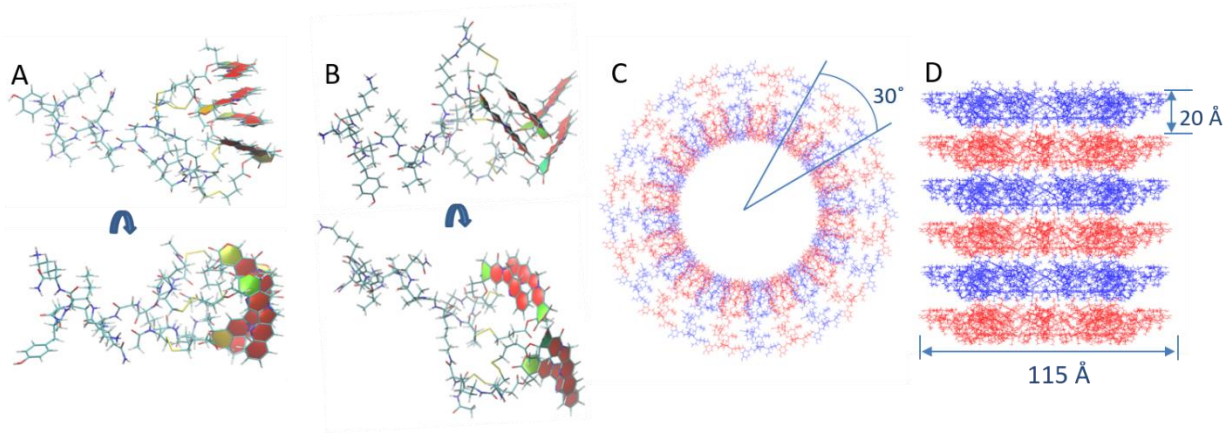

Figure S 2. Initial conformations of DA and starting structure of pre-assembled nanotube. A. The initial conformation of the DA for the nanotube A. All four CPTs are almost parallel in a DA. B. The initial conformation of the DA for the nanotube B. Two pairs of CPTs are parallel, but not altogether. C & D. Top and side view of the initial build of nanotube A. 12 DAs are placed in the first layer (blue). The CPTs are pointing inward and an angle between the neighboring DAs is 30˚. The second layer (red) has also 12 DAs and is rotated 15˚ relative to the first layer. The resulting nanotube has 6 layers with the inter-layer distance of 20 Å. The initial width of the nanotube is 115 Å. In total, it has 72 DAs.

Table S1. Preassembled systems.

System	DA/ layer	Angle between DAs, ˚	Distance between layers, Å	DA confor mation	Pressure control	Tempera ture, K	Initial width, Å	Final width, Å (time, ns)
1	9	40	18	A	isotropic	310	99.0	81.6±2.0 (409)
2 (A)	**12**	**30**	**20**	**A**	**anisotropic**	**310**	**120.6**	**104.3±3.7 (420)**
3	12	30	20	A	isotropic	310	120.6	105.4±4.5 (400)
4 (B)	**12**	**30**	**20**	**B**	**anisotropic**	**310**	**111.3**	**93.3±3.2 (400)**
5 (B_{350K})	**12**	**30**	**20**	**B**	**anisotropic**	**350**	**111.3**	**90.8±4.0 (420)**
6	12	30	20	B	anisotropic	310	138.3	125.7±8.9 (401)
7	15	24	20	A	isotropic	310	120.1	109.7±2.6 (414)

* The preassembled system 5(B_{350K}) is branched out from the preassembled system 4 after 120 ns simulation and then the temperature is elevated to 350 K for 420ns to expedite the relaxation.

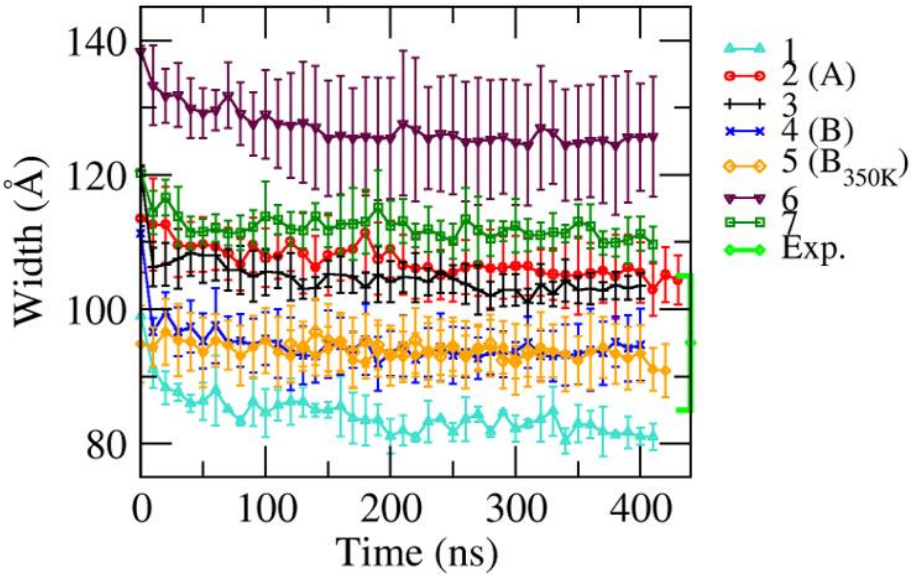

Figure S 3. Development of widths of the preassembled systems over time.

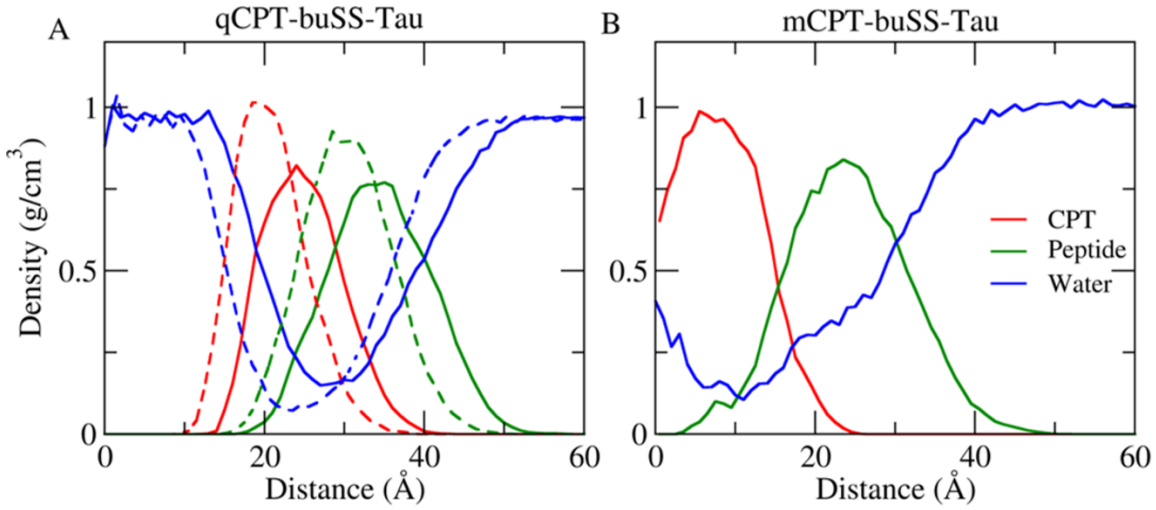

Figure S 4. Radial distribution of each component in the assembly. A. Radial density of CPT (red), peptide (green) and water (blue) in the nanotube A (solid lines) and the nanotube B (dotted lines) of qCPT-buSS-Tau. B. Radial density of CPT (red), peptide (green) and water (blue) in the nanofilament of mCPT-buSS-Tau. The width of the nanofilament of mCPT-buSS-Tau was 7.80±0.01 nm, which agreed well with the experimental width of 6.7±1 nm

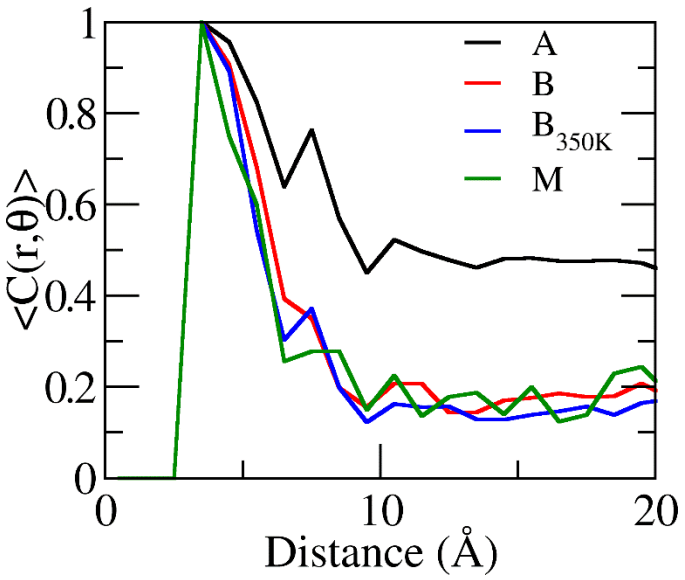

Figure S 5. Fraction of stacking over the distance between CPTs. The nanotube A, the nanotube B, the nanotube B_{350K}, and the nanofilament (M) are displayed in black, red, blue and green, respectively.

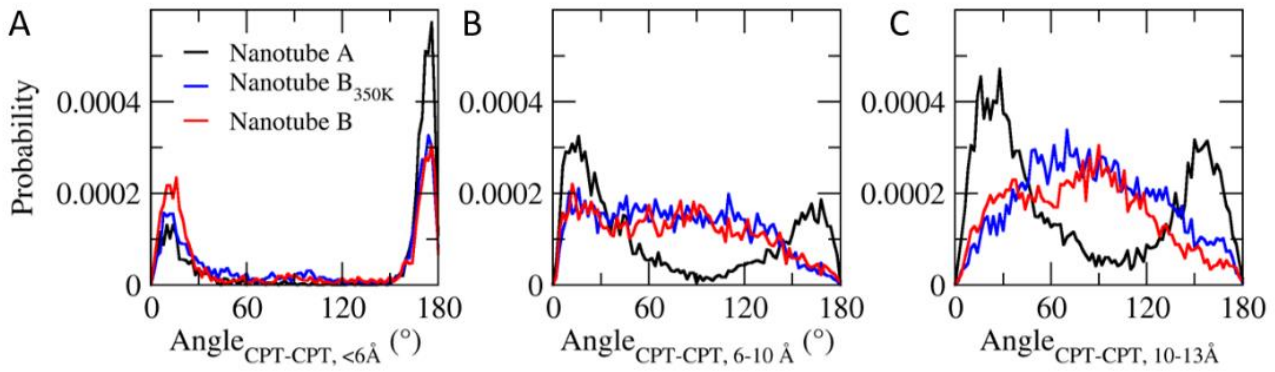

Figure S 6. The molecular stacking. A. The first stacking within 6 Å. B. The second stacking between 6 and 10 Å. C. The third stacking between 10 and 13 Å. The nanotube A, the nanotube B, and the nanotube B at 350 K are displayed in black, red and blue, respectively.

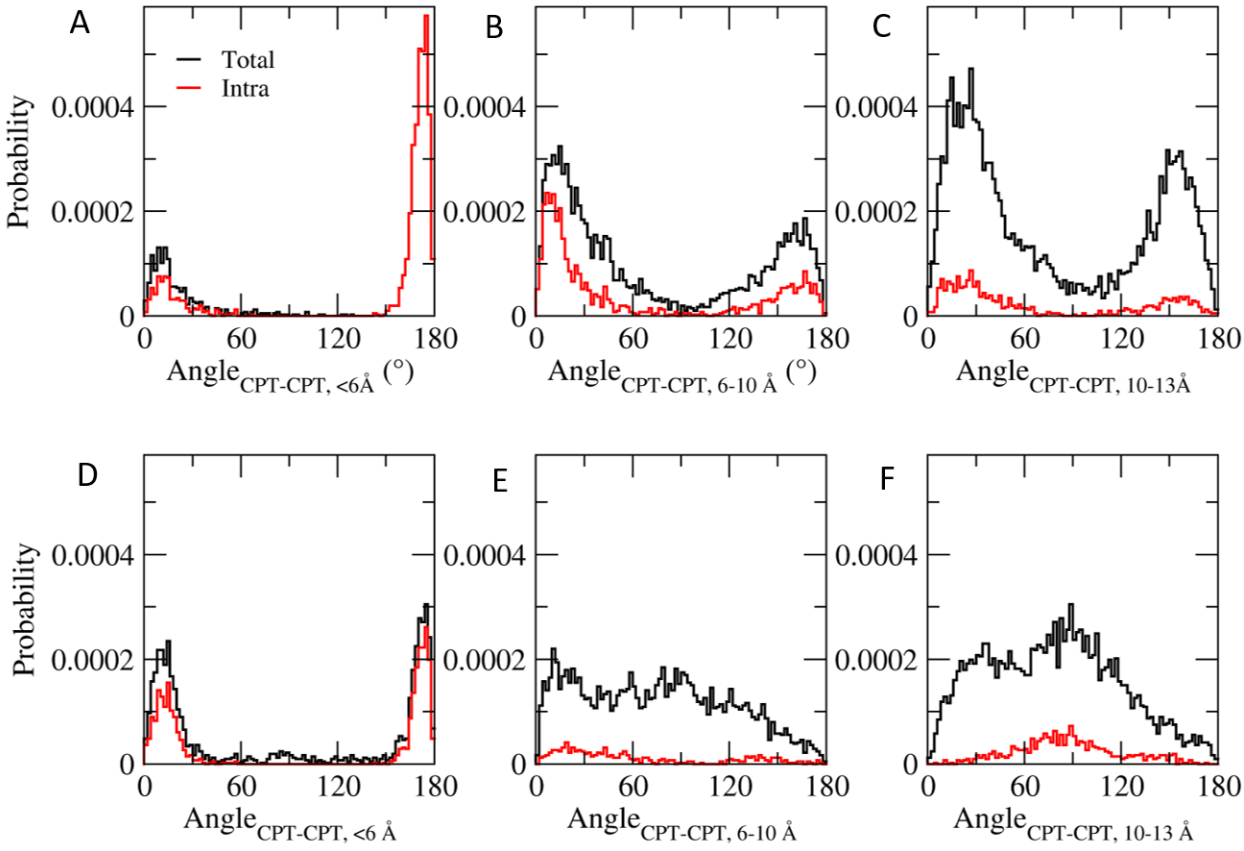

Figure S 7. The decomposition of inter-and intra-molecular stacking. A-C. Probability of angles between CPTs in the nanotube A. D-F. Probability of angles between CPTs in the nanotube B.

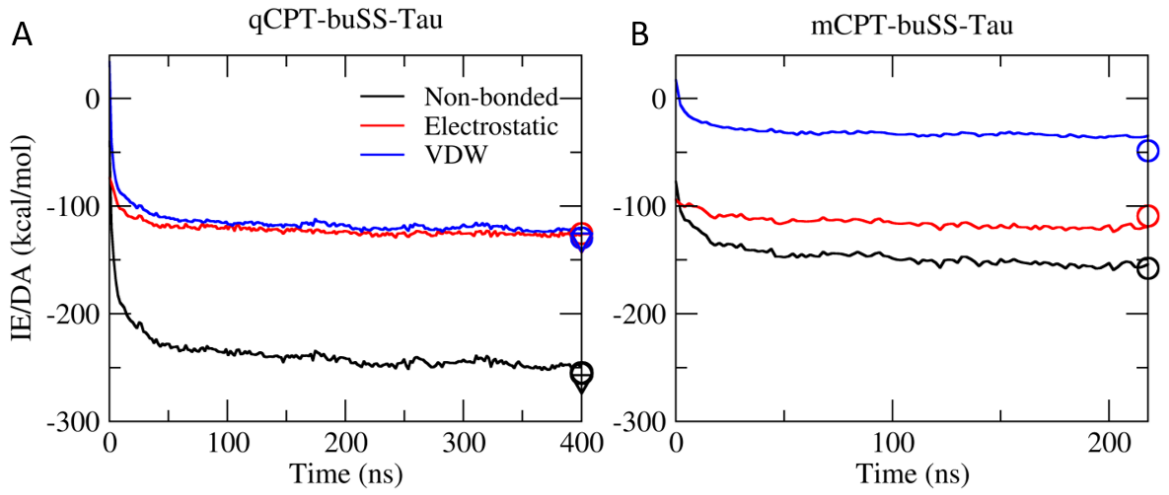

Figure S 8. Interaction energy per DA over time in the random system. A. Interaction energy per DA of qCPT-buSS-Tau. The non-bonded interaction energy (black) is decomposed into the electrostatic (red) and van der Waals contributions (blue). The corresponding energies in the preassembled nanotube A and nanotube B after 420 and 400 ns (averaged for the last 2 ns) are displayed in an empty circle and an empty triangle, respectively, with matching colors. B. Interaction energy per DA of mCPT-buSS-Tau. The corresponding energies in the preassembled nanofilament after 210 ns (averaged for the last 2 ns) is displayed in an empty circle with matching colors.

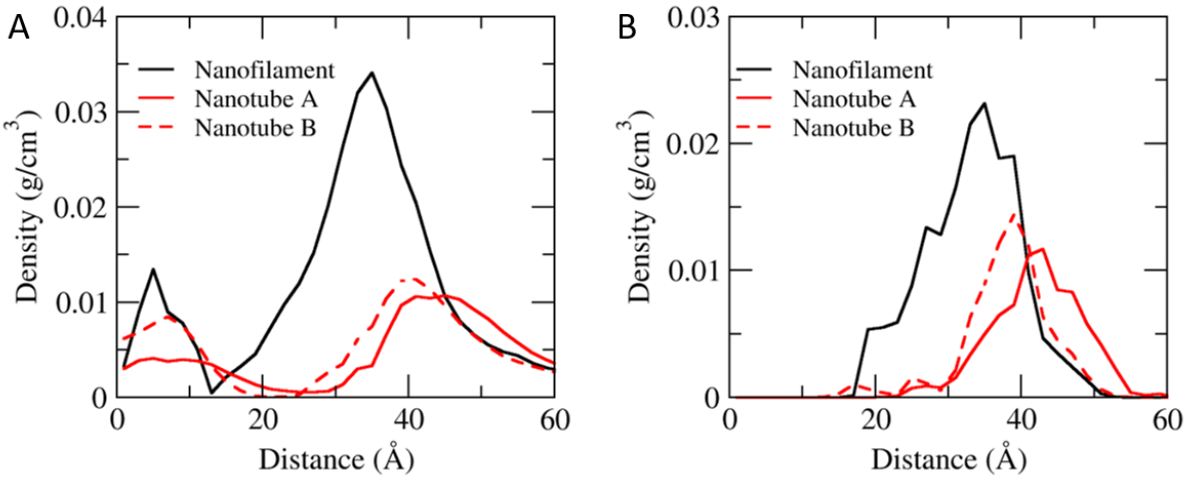

Figure S 9. Radial distribution of charge components. A. Radial distribution of Cl^- ions. The density of Cl^- ion in the nanotube A and B are in solid red and dotted red, respectively. The density of Cl^- ion in the nanofilament of mCPT-buSS-Tau (black) is displayed for comparison. B. Radial distribution of the primary ammonium ion ($-NH_3^+$) of lysine residues.

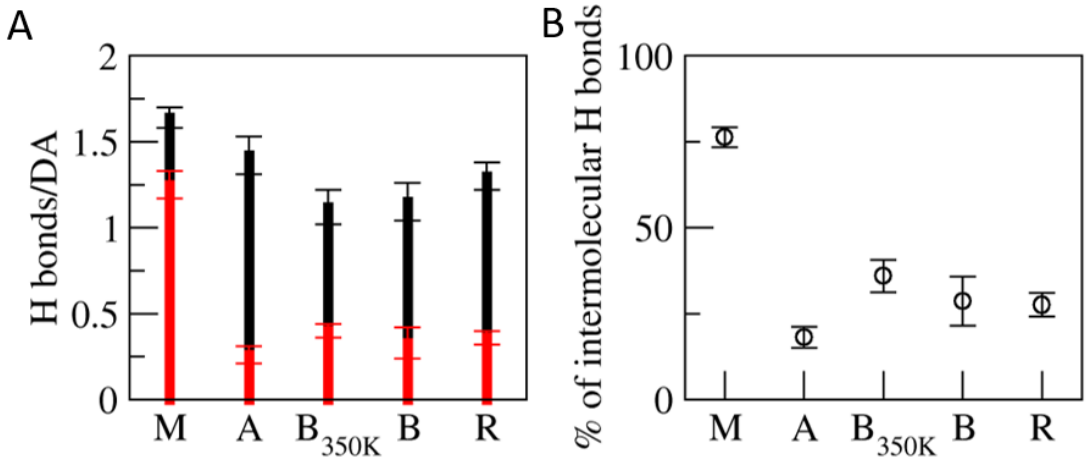

Figure S 10. Hydrogen bonds per DA. A. Numbers of hydrogen bonds per DA (black) and intermolecular hydrogen bonds (red) of the systems A, B at 350K, B, and random (R) systems at the last 2 ns. For the comparison, results from mCPT-buSS-Tau system (M) is added. B. Percent of intermolecular hydrogen bonds. [Why m has significant more intermolecular h bonds?]

References

1. Wang, J. M.; Wolf, R. M.; Caldwell, J. W.; Kollman, P. A.; Case, D. A., Development and testing of a general amber force field. *J. Comput. Chem.* **2004,** *25* (9), 1157-1174.
2. Gilson, M. K.; Gilson, H. S. R.; Potter, M. J., Fast assignment of accurate partial atomic charges: An electronegativity equalization method that accounts for alternate resonance forms. *J. Chem. Inf. Comput. Sci.* **2003,** *43* (6), 1982-1997.
3. Jorgensen, W. L.; Chandrasekhar, J.; Madura, J. D.; Impey, R. W.; Klein, M. L., COMPARISON OF SIMPLE POTENTIAL FUNCTIONS FOR SIMULATING LIQUID WATER. *J. Chem. Phys.* **1983,** *79* (2), 926-935.
4. Phillips, J. C.; Braun, R.; Wang, W.; Gumbart, J.; Tajkhorshid, E.; Villa, E.; Chipot, C.; Skeel, R. D.; Kale, L.; Schulten, K., Scalable molecular dynamics with NAMD. *J. Comput. Chem.* **2005,** *26* (16), 1781-1802.
5. Martyna, G. J.; Tobias, D. J.; Klein, M. L., Constant pressure molecular dynamics algorithms. *J. Chem. Phys.* **1994,** *101* (5), 4177-4189.
6. Feller, S. E.; Zhang, Y.; Pastor, R. W.; Brooks, B. R., Constant pressure molecular dynamics simulation: The Langevin piston method. *J. Chem. Phys.* **1995,** *103* (11), 4613-4621.
7. Darden, T.; York, D.; Pedersen, L., Particle mesh Ewald: An N·log(N) method for Ewald sums in large systems. *J. Chem. Phys.* **1993,** *98* (12), 10089-10092.
8. Andersen, H. C., Rattle: A "velocity" version of the shake algorithm for molecular dynamics calculations. *Journal of Computational Physics* **1983,** *52* (1), 24-34.
9. Ryckaert, J.-P.; Ciccotti, G.; Berendsen, H. J. C., Numerical integration of the cartesian equations of motion of a system with constraints: molecular dynamics of n-alkanes. *Journal of Computational Physics* **1977,** *23* (3), 327-341.